



Systematic identification of genes associated with plant growth–defense tradeoffs under JA signaling in *Arabidopsis*

Nailou Zhang¹ · Bin Zhao¹ · Zhijin Fan¹ · Dongyan Yang¹ · Xiaofeng Guo¹ · Qifan Wu¹ · Bin Yu¹ · Shuang Zhou¹ · Haiying Wang¹

Received: 23 October 2019 / Accepted: 21 December 2019 / Published online: 6 January 2020
© Springer-Verlag GmbH Germany, part of Springer Nature 2020

Abstract

Main conclusion Co-expression and regulatory networks yield important insights into the growth–defense tradeoffs mechanism under jasmonic acid (JA) signals in *Arabidopsis*.

Abstract Elevated defense is commonly associated with growth inhibition. However, a comprehensive atlas of the genes associated with the plant growth–defense tradeoffs under JA signaling is lacking. To gain an insight into the dynamic architecture of growth–defense tradeoffs, a coexpression network analysis was employed on publicly available high-resolution transcriptomes of *Arabidopsis* treated with coronatine (COR), a mimic of jasmonoyl-l-isoleucine. The genes involved in JA-mediated growth–defense tradeoffs were systematically revealed. Promoter enrichment analysis revealed the core regulatory module in which the genes underwent rapid activation, sustained upregulation after COR treatment, and mediated the growth–defense tradeoffs. Several transcription factors (TFs), including *RAP2.6L*, *MYB44*, *WRKY40*, and *WRKY18*, were identified as instantly activated components associated with pathogen and insect resistance. JA might rapidly activate *RAV1* and *KANI* to repress brassinosteroid (BR) response genes, upregulate *KANI*, the C2H2 TF families *ZF2*, *ZF3*, *ZAT6*, and *STZ/ZAT10* to repress the biosynthesis, transport, and signaling of auxin to arrest growth. Independent datasets and preserved analyses validated the reproducibility of the results. Our study provided a comprehensive snapshot of genes that respond to JA signals and provided valuable resources for functional studies on the genetic modification of breeding population that exhibit robust growth and defense simultaneously.

Keywords Coronatine · Coexpression network · Promoter enrichment analysis · Regulatory network · System biology

Abbreviations

BR	Brassinosteroid
COR	Coronatine
JA	Jasmonic acid
TF	Transcription factor

Electronic supplementary material The online version of this article (<https://doi.org/10.1007/s00425-019-03335-8>) contains supplementary material, which is available to authorized users.

✉ Zhijin Fan
fanzj@nankai.edu.cn

Nailou Zhang
zhangnailou@mail.nankai.edu.cn

Bin Zhao
bdzhaobin@126.com

Dongyan Yang
yangdy@nankai.edu.cn

Xiaofeng Guo
875776870@qq.com

Qifan Wu
arvinwf@foxmail.com

Bin Yu
sdjnyubin@sina.com

Shuang Zhou
1126507276@qq.com

Haiying Wang
herrynk@nankai.edu.cn

¹ State Key Laboratory of Elemento-Organic Chemistry, College of Chemistry, Nankai University, No. 94 Weijin Road, Tianjin 300071, People's Republic of China

Introduction

Plant pests and diseases affect crop production, food security and sustainable agricultural development used to meet the global food demands of a rapidly rising population (Strange and Scott 2005). Pathogen-resistant crop breeding is environmentally benign for pest management and crop protection. However, resistance genes that are adopted for resistance caused crop yield loss (Nelson et al. 2017). More than half of the studies reported that the average cost of disease resistance is less than 5% of biomass and fecundity (Bergelson and Purrington 1996). For example, the *Arabidopsis* R-gene *RPM1* costs 9% of the yield when plants are not under attack from the pathogen to which this gene confers resistance (Nelson et al. 2017). Plant defense hormones such as jasmonate (JA), ethylene (ET), salicylic acid (SA) and cytokinins play vital roles in precisely regulating plant immune responses against various pathogens (Huot et al. 2014; Naseem et al. 2015). The exogenous application of these hormones or their functional analogs to plants impairs plant normal growth (Huot et al. 2014; Naseem et al. 2015; Dubois et al. 2018; Guo et al. 2018). The molecular biology-based breeding aimed at increasing crop yield for centuries has led to the loss of plant genetic diversity and decreased plant disease resistance. It is now urgent to equip plants with advanced weapons to protect themselves against broad spectrum of pathogenic organisms without penalty of cost (Huot et al. 2014). Understanding how to balance plant growth–defense tradeoffs can provide the basis for breeding varieties that increase plant resistance and crop yield to meet growing global food demands (Huot et al. 2014). Recent studies have shown that gene stacking by simultaneously derepressing the inhibition of growth and defense or simultaneously promoting growth and defense is a promising approach to overcome the tradeoffs between defense and growth (Campos et al. 2016; Kudo et al. 2019).

A general explanation of the ‘dilemma of plants to grow or defend’ is that increased expression of defense traits consumes metabolic resources at the cost of growth, while rapid growth shifts resources that could otherwise be deployed in the defense arsenal (Campos et al. 2016). In support of this, plants under light-restrictive conditions prioritize growth and are more susceptible to *Pseudomonas syringae* and *Botrytis cinerea* attack (Huot et al. 2014). It is exceedingly difficult to measure the metabolic costs of specific defense compounds; thus, a resource-based tradeoffs model may oversimplify a highly convoluted system that is shaped by strategies aimed to balance the expense of defense (Guo et al. 2018). The second general hypothesis to explain these tradeoffs is that immune-triggered growth inhibition is an adaptive response and

regulated by hardwired interactions between growth and immune signaling networks (Guo et al. 2018).

A rising number of studies have shown that the JA pathway is a hub for integrating growth- and defense-related cues that comprehensively contribute to optimize plant fitness under adverse environmental conditions (Guo et al. 2018). JAs are a group of lipid-derived phytohormones that modulate the growth and development of plants and broad-spectrum resistance against necrotrophic pathogens and insect herbivores. Jasmonoyl-L-isoleucine (JA-Ile), the major bioactive form of the hormone, is rapidly synthesized when plants are wounded or under pathogen attack, and induces the formation of the COI1–JAZ coreceptor complex, which results in proteolytic destruction of JAZ repressors by the ubiquitin–proteasome system; this destruction derepresses several specific TFs, such as MYCs, and initiates the expression of JA-responsive genes (Huot et al. 2014). JAs also function in growth inhibition through interactions with other hormones, such as ET, auxin, BRs, and gibberellic acid (GA) (Huot et al. 2014). JAs mediate leaf growth by arresting the cell cycle in the G1 phase prior to the S transition and delaying the switch from the mitotic cell cycle to the endoreplication cycle (Huot et al. 2014). The antagonistic crosstalk between the JA and GA signaling pathways controls the growth–defense tradeoffs mediated by JAs (Guo et al. 2018). The unique combination of *jazQ* and *phyB*, which simultaneously activate MYC and PIF transcription factors, exhibits better defense than the wild type without a fitness penalty (Campos et al. 2016). The downregulation of the JA signal repressor *JAV1* results in increased resistance to both insect herbivores and necrotrophic fungi without growth penalty (Hu et al. 2013). These studies on the molecular mechanisms of JA-inducing defense-triggered growth inhibition inspired that there might be specific focal points for untangling the growth–defense tradeoffs.

With the development of high-throughput technologies such as RNA sequencing (RNA-Seq), it is now possible to assess the mode of action of phytohormones from a systematic perspective (Hickman et al. 2017). Coexpression networks and clustering algorithms can be used to construct coexpression modules in which genes have very similar expression patterns and are more likely to regulate the same biological process or function in the same pathways according to a ‘guilt-by-association’ paradigm (van Dam et al. 2018). Gene coexpression network approaches cannot be used to deduce regulatory information by itself, however, its combination with a promoter motif enrichment analysis can be performed to infer the regulatory relationships between co-expression modules and TF families (Windram et al. 2012; Hickman et al. 2017).

However, previous high-resolution time course studies of the JA response mainly revealed the chronology and regulation of the defense (Windram et al. 2012; Hickman

et al. 2017). There has never been an integrated core network that can mediate JA-induced growth arrest and defense enhancement to accurately predict genotype-by-environment interactions due to the complexity of these processes and the resource intensity of the methods to explore. Here, we performed coexpression network analysis followed by a promoter enrichment analysis with the publicly available high-resolution temporal transcriptome following JA signaling mimics treatment. We revealed that the genes associated with JA-induced defense enhancement and growth inhibition showed distinct expression patterns between mock and COR treatment. We also found that growth–defense tradeoffs mediated by JA might be regulated by different regulators in co-expression module M45. Publicly available independent datasets and a preserved analysis of module structures confirmed the robustness and reproducibility of our results. Collectively, our studies provided clues for assisting in the uncoupling of growth–defense tradeoffs and candidate genes for genetic modification in plant breeding to produce robust growth and defense simultaneously.

Materials and methods

RNA isolation and reverse-transcription quantitative PCR (RT-qPCR)

A. thaliana Columbia (Col-0), provided by Prof. Jingao Dong (Key Laboratory of Hebei Province for Plant Physiology and Molecular Pathology, Hebei Agricultural University), was used as the wild-type plant. Three-week-old *A. thaliana* plants were sprayed with 50 μM MeJA water solution. Total RNA was isolated from leaves treated with the control or MeJA, followed by cDNA synthesis using RNase-free RQ1 DNases (Promega), with the Improm-II reverse transcriptase kit (Promega) and the Oligo(dT). The expression of 18S rRNA was used to normalize the data for RT-qPCR. All primers used in this work are listed in Table S1. Data were analyzed with the $2^{-\Delta\Delta\text{CT}}$ method.

RNA-seq data analysis

The raw reads of time course expression data PRJNA245231 treated by 5 μM COR and the mock at 21 time points over a day/night cycle (16 h/8 h 22 °C/18 °C day/night) were downloaded from NCBI GEO. More details of the experiment can be found in the original report (Attaran et al. 2014).

Read processing and statistical methods were conducted by following the criteria illustrated in Fig. S1. Generally, Hisat2 v.2.0.4 (Kim et al. 2015) was used to align reads to the TAIR10. After discarding reads mapping to multiple positions in the reference, gene-level counts were computed using featurecounts (Liao et al. 2014). The genes at below

detectable levels of RNAseq in less than 80% of all samples were removed and then remained the top 30% of most variant genes. The normalized gene expression matrix was calculated using the voom normalization method in limma v.3.32.8 (Ritchie et al. 2015).

Network profiling of high-temporal resolution transcription

A signed biweight midcorrelation adjacency matrix was constructed with the power $\beta = 12$, type = “signed” and corFnc = “bicolor” using WGCNA v.1.66 (Langfelder and Horvath 2008). Then, we transformed the adjacency into a topological overlap matrix to calculate the corresponding dissimilarity. The dynamic hybrid cut method was used to cut the tree by average linkage hierarchical clustering of flashClust and identified 45 coexpression modules with minModuleSize = 20, deepSplit = 4, and cutHeight = 0.99.

Construction of regulatory relationships among modules

To explore the regulatory relationships between TFs and modules, the putative regulatory network was constructed as follows: (i) the *Arabidopsis* TF families and putative motifs bound by the TF were obtained from PlantTFDB version 4.0 (Jin et al. 2016). (ii) The known transcription factor-binding site enrichment analysis was performed by scanning 500 bp upstream of the transcription start site for the genes of each module using FIMO (Grant et al. 2011) with P value $\leq 10^{-4}$. (iii) After removing duplicated regulators of each module, the putative regulators were subjected to a hypergeometric test against the genes in each module and TF family. Significantly enriched TFs were summarized in a heatmap using ggplot2 ($\text{adj}P \leq 0.05$). (iv) Although the prediction of TF-binding sites with significant motif enrichment was considered to be a highly reliable prediction, we summarized the regulatory relationships of all module genes in PlantRegMap (Jin et al. 2015) to evaluate the core regulatory network identified by the hypergeometric analysis.

In this work, the same hypergeometric analysis was performed as in GOHyperGAll (Horan et al. 2008): $\text{phyper}(x-1, m, n-m, k, \text{lower.tail} = \text{FALSE})$. To construct the regulatory relationships between TFs and modules, x represents the number of putative regulators for each module contained in each TF family, m represents the number of genes contained in each TF family, n represents the number of all TFs, and k represents the number of putative regulators for all modules contained in all TF families. To construct the regulatory relationships among modules, x represents the number of putative regulators for each module contained in each module, m represents the number of genes in each module, n represents the number of genes in all modules, and k

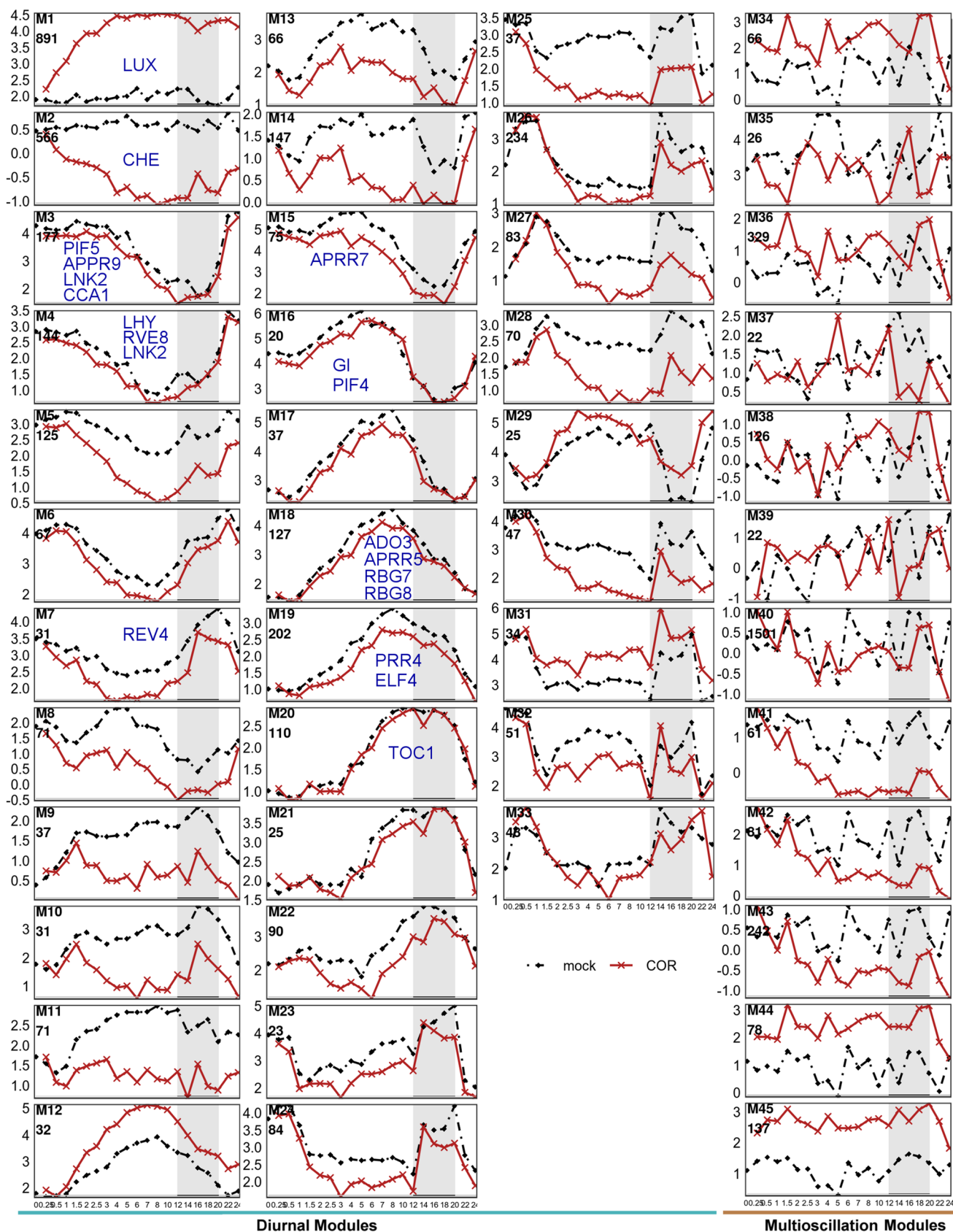


Fig. 1 Transcriptional dynamics of the 45 modules in a day/night cycle with the control and COR treatment. The black dashed lines indicate the mean expression profile of all members in the modules of the control, while the firebrick line indicates the mean expression profile of all members in the modules of COR treatment. The number of genes of each module is displayed above each panel. The gray bars denote the timing of the night in each panel. The known circadian genes are in the blue text. The y-axis indicates the mean normalized log₂ expression levels. The x-axis indicates time (h) after treatment (Table S2)

represents the number of putative regulators in all modules. The *P* value was adjusted by the Bonferroni method.

Validation experiments and preservation analyses

To test the consistency of the differential expression patterns of genes in constructed modules stimulated by different JA functional analogs, we used the publicly available transcriptomic data with MeJA treatment (Yang et al. 2017; Hickman et al. 2017) and *coi1* mutant (Yang et al. 2017). The raw fastq files were downloaded from GEO and served for the RNAseq analysis mentioned above. We assessed differential gene expression by calculating the difference between matched treatment or mutants and control samples.

Preservation analyses were performed with the gene expression data with MeJA treatment (Hickman et al. 2017). To assess the preservation of COR modules, the moduleP-reservation function in the WGCNA package was used (Langfelder et al. 2011).

Gene ontology (GO) analysis

GO functional enrichment analysis was performed using GOHyperGAll with Bonferroni-corrected *P* value (Horan et al. 2008) for all modules using the *Arabidopsis* GO annotations downloaded from the GO site (3/31/2017 release; <https://geneontology.org>). For each module, the terms with *P* value less than 0.05 were kept.

Results and discussion

Overview of the dynamic architecture of the gene coexpression network under JA signaling in a day/night cycle

A weighted gene coexpression network was constructed with a publicly available dataset treated by COR at 21 time points over a day/night cycle (Attaran et al. 2014). For this, the top 30% of most variable transcripts were selected from the filtered and normalized expression matrix, and then were used in a hierarchical clustering procedure to identify groups of coexpressed genes, termed “modules”. The high-resolution

temporal transcriptomics data captured a diverse set of dynamic responses to COR stimulation and control (Fig. 1, Fig. S2 and Table S2). Most expression changes in a day/night cycle followed two clear impulse patterns: diurnal oscillation and multioscillation (Fig. 1). Here, the genes in 33 modules that mainly peaked at one or two specific points of the day were defined as diurnal genes (Fig. 1). The amplitudes of diurnal genes were either damped or enhanced, and the global differences between the control and COR treatment were weak during the time course (e.g., M3, M18). Multioscillation genes showed more than three peaks and troughs during the time course (e.g., M34 and M40 in mock treatment). In contrast to diurnal genes, the expression of multioscillation genes, especially in M34, M36, M37, M38, and M40, not only exhibited damped or enhanced amplitude but also showed phase shifts that was significant in the night–day transition and caused dysregulation over time after COR treatment (Fig. 1). To investigate the biological significance of the distinct dynamic expression patterns, the genes in each module were tested for overrepresented functional categories using GO enrichment analysis (Fig. S3a, Table S3). The unique GO term of each module accounted for 67% of all significantly GO biological processes, and the specific GO term of each pair of modules accounted for 21% (Fig. S3b); therefore, each module might play special roles in the biological process. To detail the distribution of GO functional terms related to circadian, growth, defense, reactive oxygen species (ROS), and ion homeostasis in each module, we classified the GO terms into these four categories according to their description in web site <https://geneontology.org> (Fig. S3a, Table S3). As expected, the GO terms related to circadian or diurnal events were overrepresented in diurnal modules. The more specific functional categories were linked to distinct modules. For example, M3 was specifically enriched for the annotation term “response to light stimulus”, M4 for “response to temperature stimulus”, M15 for “photosynthesis”, and M16 for “response to temperature stimulus”. The known clock genes such as *LHY*, *CCA1*, *PRR5/7*, *TOC1*, *PCL1/LUX*, *ELF4* were also presented in diurnal modules and showed similar diurnal expression patterns as previous description (Nusinow et al. 2011; Hsu and Harmer 2014; Meyer et al. 2017) (Fig. 1 and Table S2), indicating that the dynamic expression profiles we captured using coexpression network were reproducible and robust. The GO terms associated with ROS and “ion homeostasis” were mainly presented in multioscillation modules (Fig. S3a). For example, M35 was specifically enriched for the annotation term “reactive oxygen species metabolic process” and “iron ion homeostasis”, M40 for “ion homeostasis” and “oxidation–reduction process”, M41 for “cellular response to metal ion”, and M43 for “zinc II ion transport” and “hydrogen peroxide catabolic process” (Table S3). Remarkably, after mapping all genes to corresponding chromosome

locations, we found 19 chloroplast chromosome genes in M37, which was composed of 22 genes (Fig. S2). *psaA*, *psaB*, and *psbA*, the critical components of photosystem I and photosystem II (Schult et al. 2007; Krech et al. 2012), were also in this module. Therefore, the modules we constructed provided a general picture of the relevant biological processes and might assist future functional characterization experiments of genes of unknown functions related to circadian rhythm, photosynthesis, and multioscillation.

We externally validated the robustness of our findings by determining whether the modules detected in the COR dataset were preserved in publicly available MeJA datasets (Hickman et al. 2017). The results suggested that most modules showed evidence for moderate preservation between COR and MeJA treatments (Fig. S4; Zsummary > 2).

Gradually activated genes associated with defense enhancement mediated by JA

Here, we found that the genes in module M1 exhibited two distinct expression patterns following the control and COR treatment (Fig. 1, Fig. S2). The genes in M1 showed the diurnal expression pattern during the day/night cycle following mock treatment, while these genes were rapidly upregulated in the first 4 h and maintained the status of consecutive activation at least throughout the time course after treatment with COR (Fig. 1, Fig. S2). This module was enriched for functional terms associated with JA defense responses (Fig. S3a), and most of the genes annotated with “response to wounding” and “responding to jasmonic acid” were included in this module (Fig. S2). Interestingly, the defense module not only contained JA biosynthesis genes and known pathogen- and herbivory-responsive marker genes, such as *AOS*, *AOC2*, *LOX2*, *OPR3*, *PDF1.2A*, *VSP2* and *ORA47*, but also contained JA negative feedback genes and JA signal repressors, such as JAZ proteins (*JAZ1/2/3/4/5/6/7/8/9/10/12/13*) and jasmonate-induced oxygenases (*JOX1/2/3/4*), which hydroxylated JA to form inactive 12-OH-JA (Caarls et al. 2017). DELLA proteins *RGL3* and *RGL2* and circadian genes *LUX* were also presented in this module (Fig. 3). Convincingly, the expression patterns of JAZs after MeJA treatment were consistent with the previous report (Thines et al. 2007).

COR is a structural mimic of JA-Ile and acts directly as an antagonist of the COI1-JAZ co-receptor, thereby specifically activating the JA signaling pathway (Attaran et al. 2014). To validate that the genes in M1 had similar differential expression patterns during COR or MeJA stimulation, the differential gene expression profiles stimulated by COR were compared to those of two independent MeJA-treated RNA-Seq datasets (Yang et al. 2017; Hickman et al. 2017). As expected, the differential gene expression patterns in M1

stimulated by COR were fairly similar to those under MeJA treatment (Fig. 2).

The F-box protein COI1 is identified as a major component of the JA pathway, as loss of *COI1* function resulted in compromised resistance to necrotrophic fungi and herbivorous insects; *coi1* mutants did not respond to JA treatment and impaired the expression of most JA- and insect-inducible genes (Goossens et al. 2016). Here, the RNA-Seq dataset of the *coi1-16* mutants (Yang et al. 2017) was used to test whether the genes activated by JA signaling were dependent on *COI1*. Many genes in M1, including JA-responsive genes *LOX3*, *LOX4*, *AOS*, *AOC1*, *OPR3*, *PDF1.2A*, *VSP1*, and JAZs (Fig. 2), were repressed in *coi1* mutants. Collectively, these results indicated that the genes in M1 were associated with the defense mediated by JAs and provided clues for discovering many defense molecular mechanisms related to *COI1* under JA signaling.

Gradually downregulated genes associated with growth arrest under JA signaling

It has long been recognized that triggering JA signaling by applying JA to the growth medium results in growth repression (Huot et al. 2014). Leaf growth is rapidly inhibited after COR treatment (Attaran et al. 2014). Here, we found that the genes in M2 were gradually downregulated in the first 12 h and were repressed over time after treatment with COR (Fig. 1, Fig. S2). However, the control exhibited only a slight fluctuation in basal expression during the day/night cycle (Fig. 1). These genes showed similar differential expression patterns when stimulated by MeJA or COR (Fig. 2). As expected, this module was enriched for functional terms associated with growth, such as “response to auxin” (Fig. S3a). There were many genes involved in the biosynthesis, transport, and signaling of auxin presented in this module. For example, *PLT7* modulated local auxin biosynthesis in the center of the meristem (Pinon et al. 2013); *SAUR50/64/66*, *IAA19/34*, and *ATIG48660* belonged to the three families of early auxin-responsive genes—small auxin-up RNA (SAUR), Aux/IAA, and GH3, respectively. These three families could be specifically induced by auxin within minutes (Paponov et al. 2008). *ARF11/18* were auxin response factors (ARF), which might modulate the expression of genes by binding to the promoter regions of auxin-responsive genes and amplify the auxin signal. *PIN5* was a functional auxin transporter and regulated intracellular auxin homeostasis and metabolism (Mravec et al. 2009). Additional inspections revealed that there were other growth-related genes shown in this module, such as the GA-related genes: *GASA6*, *PRE5*, and *HBII*; the BR marker gene: *EXP8*; the cell expansion genes: *EXPA11*, *EXPA5*, and *EXPA1*; and the genes involved in cell differentiation: *PRK4*, *TCLI*, and *ETC2* (Fig. 2).

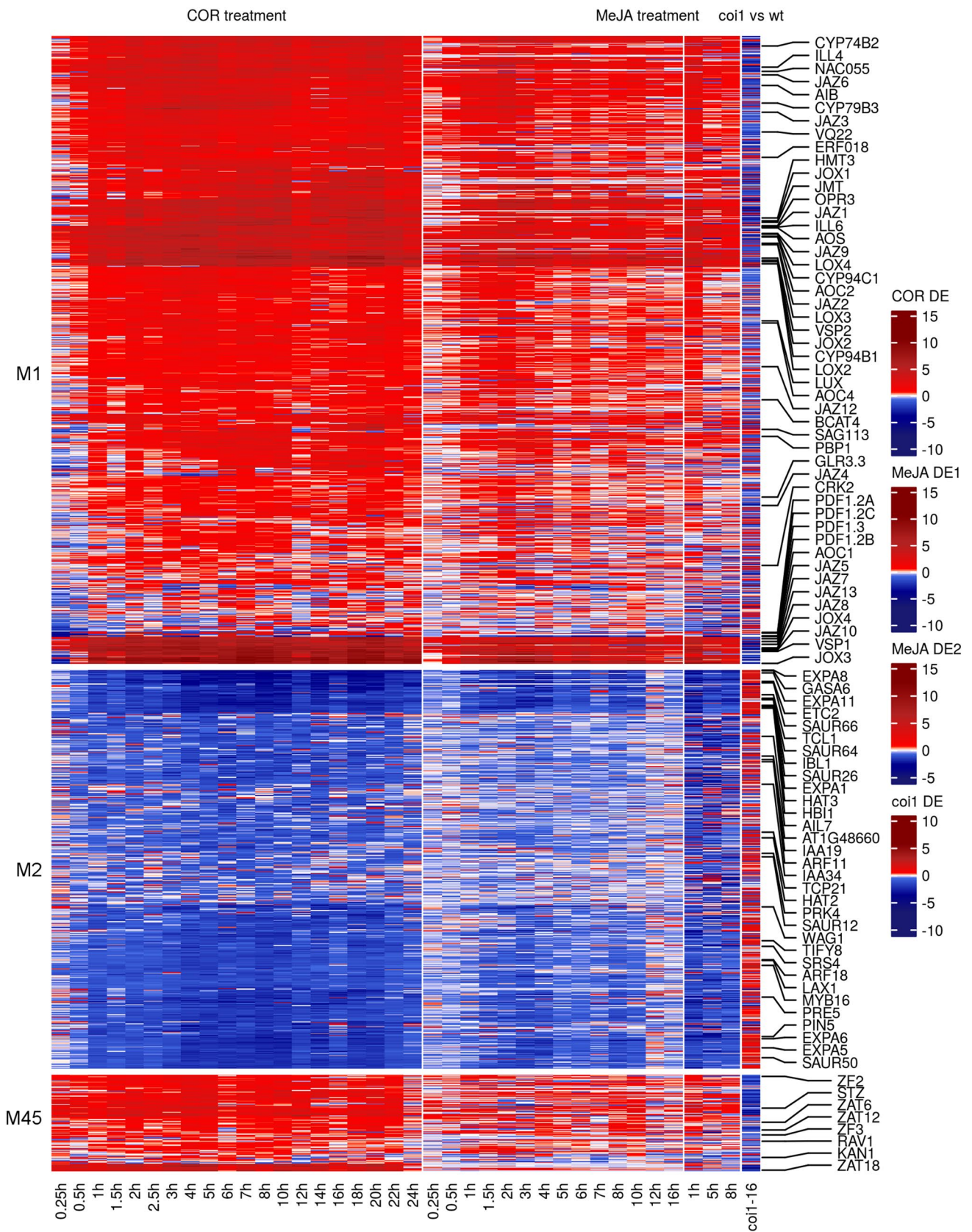
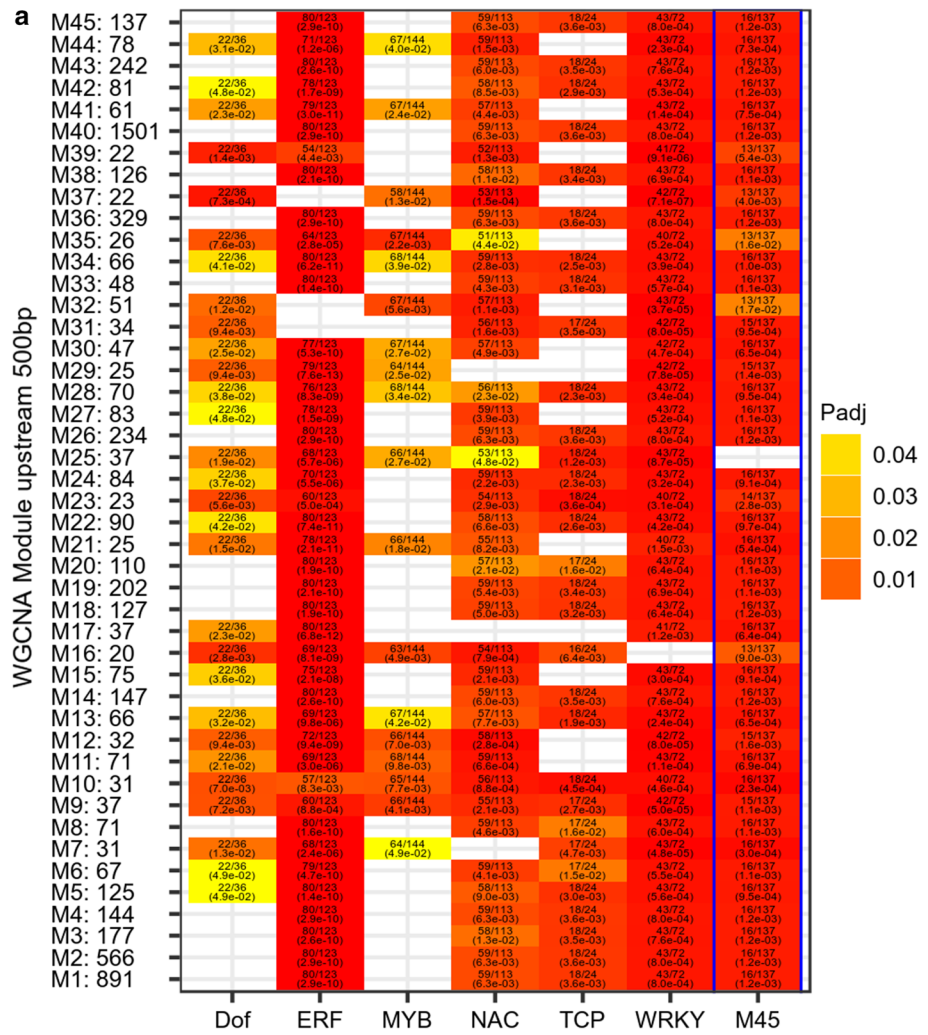


Fig. 2 The comparison of differential expression profiles responding to COR and MeJA. The differential expression patterns in M1, M2 and M45 modules in response to COR, MeJA, and *coi1* mutants. The legends indicate the differential expression levels

Fig. 3 The regulatory relationships between co-expression modules and TFs. **a** The regulators in TF families and M45 significantly overrepresented in the putative regulators of each module determined by promoter motif analysis. Numbers (N1/N2) in the table report the number (N1) of the putative regulators for each module contained in each TF family or in M45 and the number (N2) of members of TF family or M45, with the corrected *P* value printed below the numbers in parentheses. **b** The regulatory relationships count of co-expression modules in PlantRegMap. The number represents the count of genes in PlantRegMap regulated by TFs in each module



In addition to its well-documented importance for biotic stress responses, *COI1* also mediates signal transduction in light-driven developmental processes. The growth of *Arabidopsis coil* mutants and *COI1*-silenced rice plants is enhanced when compared to the respective wild-type plants (Goossens et al. 2016). Under conditions of competition

with neighbors, at a low ratio between red and far-red light, hypocotyls of *coil* mutants elongate more than those of wild-type plants (Goossens et al. 2016). The *coil-30* mutants invalidate the impact of COR treatment on growth (Attaran et al. 2014). To test whether the genes repressed by JA signaling were upregulated in *coil* mutants, we explored

the differential expression levels of these genes in *coil-16*. As shown in Fig. 2, many genes related to growth, such as *ATIG48660*, *SAUR50* and *HAT3*, were upregulated in *coil* mutants and repressed by MeJA or COR. Therefore, these findings might help elucidate the molecular mechanisms of JA-induced growth arrest.

Discovery of the core for regulating growth–defense tradeoffs under JA signaling

TFs regulate gene expression by binding to specific sequences in the promoter regions of their target genes (Chang et al. 2006), and the information of the regulatory DNA motifs that are associated with genes in each module could aid in the understanding of the regulatory relationship among modules. We performed a promoter enrichment analysis on the genes of each module using FIMO, which searches a set of sequences for occurrences of known motifs (Grant et al. 2011), on the basis of DNA-binding specificities from PlantTFDB 4.0 (Jin et al. 2016). Then, the hypergeometric test was utilized to assess the putative regulators overrepresented against all TFs categories, motifs corresponding to DNA-binding sites of ERF, NAC and WRKY TFs were found to be enriched in almost all modules (Fig. 3a). Hypergeometric test was utilized to assess the putative regulators overrepresented against genes in each module, only motifs corresponding to the DNA-binding sites of TFs in M45 were markedly enriched in all modules except for those in M25. We mapped genes in all modules to PlantRegMap, composed of genome-wide regulatory interactions curated from the literature and inferred by combining TF-binding motifs and regulatory elements (Jin et al. 2015). 18 TFs in M45 had 24, 111 regulatory relationships with other genes in PlantRegMap (Fig. 3b and Table S4) and accounted for 80% of the regulatory relationships in all co-expression modules. These suggested that the regulators in M45 regulated all modules except for M25. In addition, M45 was composed of 137 genes, including 26 TFs, 7 lncRNAs, 1 snoRNA and 37 putative uncharacterized proteins or unannotated genes (Table S2).

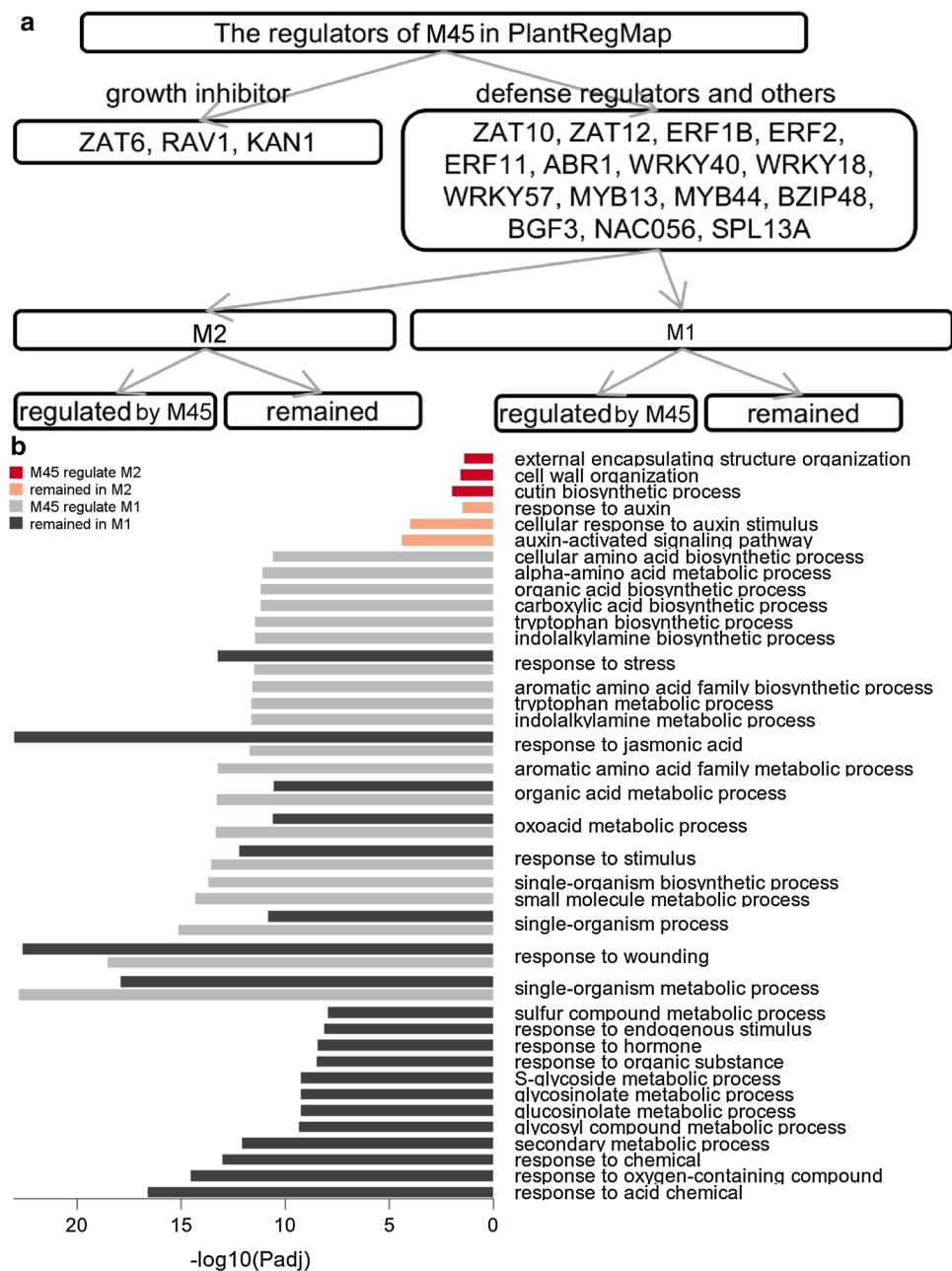
M45 was overrepresented for functional terms associated with defense, ROS, growth, and development (Fig. S3a, Fig. S2). The genes in this module were rapidly activated within 15 min and then maintained consecutive activation after COR or MeJA treatment (Figs. 1, 2). Considering the differential expression patterns of the gradually activated defense (M1), the gradually repressed growth (M2) (Figs. 1, 2) and the results of a promoter enrichment analysis mentioned above, we suggested that this module mediated the antagonistic interaction between growth and defense mediated by JA signaling. To validate this hypothesis, we investigated the regulatory relationships between this module and M1 (defense) or M2 (growth) in PlantRegMap (Fig. 4a). 172

genes of M2 regulated by 15 TFs were annotated as non-growth inhibitors in M45, and were enriched for GO term “cell wall organization” under the corrected *P* value of 0.05 (Fig. 4). On the other hand, the remaining 394 genes in M2 were enriched for growth-related GO terms such as “auxin-activated signaling pathway” (Fig. 4b). Genes in the M1 were regulated by M45’s defense regulators and those that remained in M1 were enriched by defense-related GO terms (Fig. 4b). There were no significantly enriched GO terms in M2 or M1 under the regulation of M45’s growth inhibitors, because these growth inhibitors had few regulatory relationships in PlantRegMap. These suggested that growth–defense tradeoffs mediated by JA might be regulated by different regulators in M45, rather than just mediated by molecular switch like JAZ-DELLA.

Among the TFs in M45, *KANI*, *RAVI*, *STZ/ZAT10*, *ZAT6*, and *ERF11* physically interact in yeast with the TOPLESS corepressor protein (Causier et al. 2011). Thus, *KANI*, *RAVI*, *STZ/ZAT10* and *ZAT6* might cause repression by interacting with TOPLESS, thereby recruiting chromatin-repressive enzymes. *KANI* is a transcriptional repressor that regulate auxin biosynthesis, transport, and signaling (Huang et al. 2014; Xie et al. 2015). In M2, the activator *HBII* positively regulates BR biosynthesis of two expansion genes, *EXPA1* and *EXPA8*, that encode cell wall-loosening enzymes (Fan et al. 2014); and the auxin-signaling genes *HAT2* and *AT5G12050* are putative *KANI* targets supported by the ChIP-seq and tiling array approaches (Merelo et al. 2013). Overexpressing *RAVI* provokes retardation of lateral root and rosette leaf development in *Arabidopsis* (Hu et al. 2004). *RAVI* is also a representative gene for BR upregulation (Hu et al. 2004). *AZF2*, *AZF3*, *ZAT6*, *STZ/ZAT10*, and *ZAT12* belong to the C1-2i subclass family of C2H2 zinc finger TFs in *Arabidopsis* and are highly induced by cold, osmotic, salt, drought, UV-B, and wounding in shoot tissue (Yin et al. 2017). It was well shown that the C2H2 zinc finger families play essential roles in the growth inhibition response to various a/biotic stresses (Ciftci-Yilmaz et al. 2007; Kodaira et al. 2011; Yin et al. 2017). *AZF2* negatively regulated auxin-inducible genes under abiotic stress conditions (Kodaira et al. 2011). The double mutant *azf1azf2* tended to show delayed chlorosis or enhanced root growth and increased levels of small auxin-up RNA gene expression when compared with wild-type plants under high-salt conditions (Kodaira et al. 2011). Overexpression of *ZAT6* showed pleiotropic phenotypes with curly leaves and small-sized plants at the vegetative stage, reduced floral organ and silique sizes at the reproductive stage, and improved resistance to biotic and abiotic stresses (Shi et al. 2014). The consecutive expression of *STZ/ZAT10* was found to result in growth retardation and improved adaptation of plants to a/biotic stresses (Shi et al. 2014). *AZF3* and *ZAT12* were also identified as transcription repressors (Sakamoto et al. 2004; Li et al. 2018). The

Fig. 4 The growth (M2) and defend (M1) modules are regulated by different TFs of M45.

a The TFs of M45 in PlantRegMap are grouped as growth inhibitors and non-growth suppressors; **b** The red bars display the GO process of genes of M2 regulated by regulators associated with the defense of M45 in PlantRegMap. The pink bars display the GO process of remaining genes of M2 unregulated by regulators of M45. The gray bars display the GO process of genes of M1 regulated by regulators associated with the defense of M45 in PlantRegMap. The black bars display the GO process of the remaining genes of M1 unregulated by regulators of M45. The description of the top 20 significantly GO terms is shown on the left of bars. The x-axis displays the corrected significant P value



knockout of *ZAT12* had a positive effect on growth under heat stress (Davletova et al. 2005). Real-time RT-qPCR analysis showed the strong activation of *KAN1*, *RAV1*, and the C2H2 TFs *AZF1*, *AZF2*, *AZF3*, *ZAT6*, *STZ/ZAT10*, and *ZAT12* when treated with MeJA (Fig. 5). *ERF11* overexpression induced *GA2-OX6*, encoding a GA degradation enzyme, in leaves and hence inhibited leaf growth (Dubois et al. 2018). Based on the above observations, a working model was proposed in Fig. 6 to describe the mechanism of immune-triggered growth inhibition mediated by JA signals on leaves. In addition to the well-documented crosstalk of GA and JA to balance plant–defense tradeoffs, we found that JA might rapidly activate *RAV1* and *KAN1* to repress BR

response genes, upregulate *KAN1*, the C2H2 TF families *ZF2*, *ZF3*, *ZAT6*, and *STZ/ZAT10* to repress the biosynthesis, transport, and signaling of auxin to arrest growth. These results might shed light on the molecular mechanism underlying the crosstalk between JA signaling and growth.

On the other hand, *ERF1B* (in M45) could directly upregulate *ASA1* (in M1) by binding to its promoter, leading to auxin accumulation and ET-induced root growth inhibition (Mao et al. 2016). *WRKY57* mediated the antagonism of JA- and auxin-mediated signaling in leaf senescence process (Jiang et al. 2014) and has a dual role in a/biotic stress (Jiang et al. 2014; Jiang and Yu 2016). The C2H2 TFs (*ZF2*, *ZF3*, *ZAT6*, *STZ/ZAT10*, *ZAT12*, and *ZAT18*), the ERF TFs

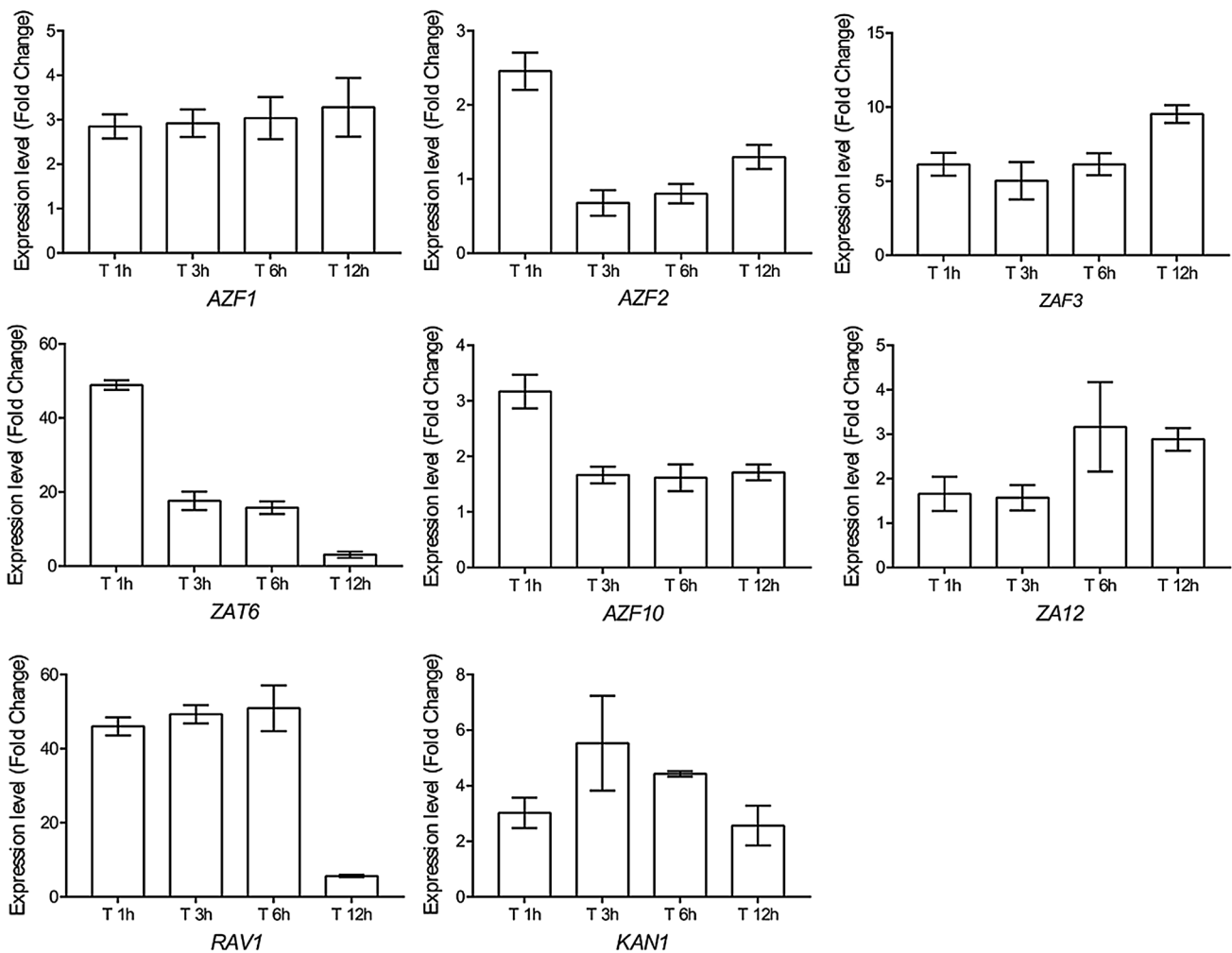


Fig. 5 RT-qPCR transcript profiles for eight TFs verifying the transcriptional data

(*ERF1B*, *ERF2*, and *ERF113/RAP2.6L*), the WRKY TFs (*WRKY40*, and *WRKY18*), and the NAC TF *NAC056* played positive central roles in a/biotic stresses (Sakamoto et al. 2000; He et al. 2005; McGrath et al. 2005; Pandey et al. 2010; Krishnaswamy et al. 2011; Xie et al. 2012; Liu et al. 2013; Cheng et al. 2013; Yin et al. 2017). These genes were repressed in the *coi1* mutant (Fig. 2). Thus, JA signals might rapidly and consecutively activate these C2H2 TFs as well as *KAN1* and *RAV1* to arrest growth, and activate *ERF1B*, *ERF2*, *ERF113/RAP2.6L*, *WRKY18*, *WRKY40*, *WRKY57*, and *ZAT18* to enhance defense through *COI1*.

Gene coexpression networks organized genes with similar expression patterns. A specific family of TFs might regulate the genes within a coexpression module. Thus, it was possible to identify the regulatory relationships between the coexpression modules and TFs by studying a specific motif's distribution across the network (Vandepoele et al. 2009). Coupling TF DNA-binding motif enrichment data with the chronological JA network model predicted putative causal

regulatory relationships between TFs and JA-regulated modules (Hickman et al. 2017). By integrating cumulative hypergeometric distribution test with promoter motif enrichment data of genes in each constructed module, the TFs in M45 were predicted for playing vital roles in regulating the antagonism between growth and defense (Fig. 3). Indeed, the regulatory relationships among genes in PlantRegMap also confirmed that the TFs in M45 were important in the transcriptional regulatory network (Figs. 3 and 4). Therefore, we performed a robust approach that was useful for inferring regulatory relationships among co-expression modules.

Conclusions

Understanding the mechanisms of growth–defense trade-offs is critical for breeding resistant plants for higher yields. Using a coexpression network analysis following hierarchical clustering on a high-resolution RNA-seq time

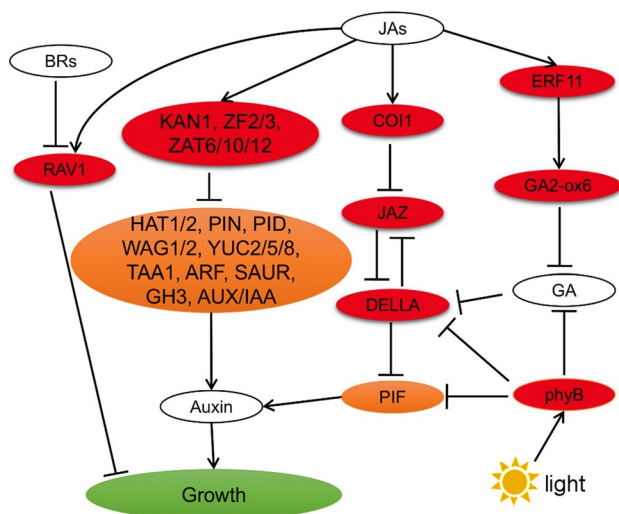


Fig. 6 Model depicting the mechanism of growth inhibition under JA signals. JA could rapidly induce the expression of growth inhibitors (*RAV1*, *KAN1*, *ZF2/3*, *ZAT6/10/12*, *ERF11*) and arrest growth through crosstalk with BRs, auxin and GA. Light-activated *phyB* binds to and degrades *PIF4/5*

series treated by COR and validating with independent data, we provided an unprecedentedly detailed insight into the architecture and dynamics of gene expression in a day/night cycle with the control and JA signal treatment, and systematically revealed the genes associated with antagonism between growth and defense mediated by JA signaling. The genes in the core regulatory module, inferred by a promoter enrichment analysis, would be candidates for unlinking growth–defense tradeoffs. Our results were only based on publicly available transcriptomes of *Arabidopsis* treated with JA analogs. Biotic stress such as the attack from herbivory insects and necrotrophic pathogens (such as *Botrytis cinerea*) might trigger different transcriptomic responses. Hence, interpretation of these results might need to consider other factors affecting transcription. Future research will be focused on biological validation of candidate genes with putative regulatory roles in mediating JA-triggered growth–defense tradeoffs. Knowledge on how plants optimize plant fitness under adverse environmental conditions will aid in breeding disease-resistant crops without growth penalty.

Availability of data and materials

All data generated or analyzed during this study are included in this published article [and its Additional files].

Acknowledgements This paper was dedicated to The 100th Anniversary of Nankai University and The 100th Birthday Anniversary of Professor Ruyu Chen.

Author contributions ZF and NZ conceived the original research plan; NZ analyzed the data, performed statistical analyses, data visualization, and wrote the manuscript; BZ performed RT-qPCR experiments. BZ, DY, XG, QW, BY, SZ, and HW authored or reviewed drafts of the paper. All authors read and approved the final manuscript.

Funding This work was supported in part by the National Key Research & Development Program of China (No. 2017YFD0200900 and No. 2017YFD0200903), the National Natural Science Foundation of China (No. 31872007 and No. 31571991), the Tianjin Natural Science Foundation (No. 18JCZDJC33500), the International Science & Technology Cooperation Program of China (No. 2014DFR41030) and The Fundamental Research Funds for the Central Universities, Nankai University (No 63191743 and No 63191323).

Compliance with ethical standards

Conflict of interest The authors declare that they have no competing interests.

References

- Attaran E, Major IT, Cruz JA et al (2014) Temporal dynamics of growth and photosynthesis suppression in response to jasmonate signaling. *Plant Physiol* 165:1302–1314. <https://doi.org/10.1104/pp.114.239004>
- Bergelson J, Purrington CB (1996) Surveying patterns in the cost of resistance in plants. *Am Nat* 148:536–558. <https://doi.org/10.1086/285938>
- Caarls L, Elberse J, Awwanah M et al (2017) *Arabidopsis* jasmonate-induced oxygenases down-regulate plant immunity by hydroxylation and inactivation of the hormone jasmonic acid. *Proc Natl Acad Sci USA* 114:6388–6393. <https://doi.org/10.1073/pnas.1701101114>
- Campos ML, Yoshida Y, Major IT et al (2016) Rewiring of jasmonate and phytochrome B signaling uncouples plant growth–defense tradeoffs. *Nat Commun* 7:12570. <https://doi.org/10.1038/ncomms12570>
- Causier B, Ashworth M, Guo W, Davies B (2011) The TOPLESS interactome: a framework for gene repression in *Arabidopsis*. *Plant Physiol* 158:423–438. <https://doi.org/10.1104/pp.111.186999>
- Chang L-W, Nagarajan R, Magee JA et al (2006) A systematic model to predict transcriptional regulatory mechanisms based on overrepresentation of transcription factor binding profiles. *Genome Res* 16:405–413. <https://doi.org/10.1101/gr.4303406>
- Cheng M-C, Liao P-M, Kuo W-W, Lin T-P (2013) The *Arabidopsis* ethylene-response-Factor1 regulates abiotic-stress-responsive gene expression by binding to different cis-acting elements in response to different stress signals. *Plant Physiol* 162:1566–1582. <https://doi.org/10.1104/pp.113.221911>
- Ciftci-Yilmaz S, Morsy MR, Song L et al (2007) The ear-motif of the C2H2 zinc-finger protein ZAT7 plays a key role in the defense response of *Arabidopsis* to salinity stress. *J Biol Chem* 282:9260–9268. <https://doi.org/10.1074/jbc.M611093200>
- Davletova S, Schlauch K, Coutu J, Mittler R (2005) The zinc-finger protein ZAT12 plays a central role in reactive oxygen and abiotic stress signaling in *Arabidopsis*. *Plant Physiol* 139:847–856. <https://doi.org/10.1104/pp.105.068254>

- Dubois M, Van den Broeck L, Inzé D (2018) The pivotal role of ethylene in plant growth. *Trends Plant Sci* 23:311–323. <https://doi.org/10.1016/j.tplants.2018.01.003>
- Fan M, Bai M-Y, Kim J-G et al (2014) The bHLH transcription factor HB11 mediates the trade-off between growth and pathogen-associated molecular pattern-triggered immunity in *Arabidopsis*. *Plant Cell* 26:828–841. <https://doi.org/10.1105/tpc.113.121111>
- Goossens J, Fernández-Calvo P, Schweizer F, Goossens A (2016) Jasmonates: signal transduction components and their roles in environmental stress responses. *Plant Mol Biol* 91:673–689. <https://doi.org/10.1007/s11103-016-0480-9>
- Grant CE, Bailey TL, Noble WS (2011) FIMO: scanning for occurrences of a given motif. *Bioinformatics* 27:1017–1018. <https://doi.org/10.1093/bioinformatics/btr064>
- Guo Q, Major IT, Howe GA (2018) Resolution of growth–defense conflict: mechanistic insights from jasmonate signaling. *Curr Opin Plant Biol* 44:72–81. <https://doi.org/10.1016/j.pbi.2018.02.009>
- He X-J, Mu R-L, Cao W-H et al (2005) AtNAC2, a transcription factor downstream of ethylene and auxin signaling pathways, is involved in salt stress response and lateral root development. *Plant J* 44:903–916. <https://doi.org/10.1111/j.1365-313X.2005.02575.x>
- Hickman R, Verk MCV, Dijken AJHV et al (2017) Architecture and dynamics of the jasmonic acid gene regulatory network. *Plant Cell* 29:2086–2105. <https://doi.org/10.1105/tpc.16.00958>
- Horan K, Jang C, Bailey-Serres J et al (2008) Annotating genes of known and unknown function by large-scale coexpression analysis. *Plant Physiol* 147:41–57. <https://doi.org/10.1104/pp.108.117366>
- Hsu PY, Harmer SL (2014) Wheels within wheels: the plant circadian system. *Trends Plant Sci* 19:240–249. <https://doi.org/10.1016/j.tplants.2013.11.007>
- Hu YX, Wang YH, Liu XF, Li JY (2004) *Arabidopsis* RAV1 is down-regulated by brassinosteroid and may act as a negative regulator during plant development. *Cell Res* 14:8–15. <https://doi.org/10.1038/sj.cr.7290197>
- Hu P, Zhou W, Cheng Z et al (2013) JAV1 controls jasmonate-regulated plant defense. *Mol Cell* 50:504–515. <https://doi.org/10.1016/j.molcel.2013.04.027>
- Huang T, Harrar Y, Lin C et al (2014) *Arabidopsis* KANADII acts as a transcriptional repressor by interacting with a specific cis-element and regulates auxin biosynthesis, transport, and signaling in opposition to HD-ZIPIII factors. *Plant Cell* 26:246–262. <https://doi.org/10.1105/tpc.113.111526>
- Huot B, Yao J, Montgomery BL, He SY (2014) Growth–defense tradeoffs in plants: a balancing act to optimize fitness. *Mol Plant* 7:1267–1287. <https://doi.org/10.1093/mp/ssu049>
- Jiang Y, Yu D (2016) The WRKY57 transcription factor affects the expression of jasmonate ZIM-domain genes transcriptionally to compromise *Botrytis cinerea* resistance. *Plant Physiol* 171:2771–2782. <https://doi.org/10.1104/pp.16.00747>
- Jiang Y, Liang G, Yang S, Yu D (2014) *Arabidopsis* WRKY57 functions as a node of convergence for jasmonic acid- and auxin-mediated signaling in jasmonic acid-induced leaf senescence. *Plant Cell* 26:230–245. <https://doi.org/10.1105/tpc.113.117838>
- Jin J, He K, Tang X et al (2015) An *Arabidopsis* transcriptional regulatory map reveals distinct functional and evolutionary features of novel transcription factors. *Mol Biol Evol* 32:1767–1773. <https://doi.org/10.1093/molbev/msv058>
- Jin J, Tian F, Yang D-C et al (2016) PlantTFDB 4.0: toward a central hub for transcription factors and regulatory interactions in plants. *Nucleic Acids Res* 45:D1040–D1045
- Kim D, Langmead B, Salzberg SL (2015) HISAT: a fast spliced aligner with low memory requirements. *Nat Methods* 12:357–360. <https://doi.org/10.1038/nmeth.3317>
- Kodaira K-S, Qin F, Tran L-SP et al (2011) *Arabidopsis* Cys2/His2 zinc-finger proteins AZF1 and AZF2 negatively regulate abscisic acid-repressive and auxin-inducible genes under abiotic stress conditions. *Plant Physiol* 157:742–756. <https://doi.org/10.1104/pp.111.182683>
- Krech K, Ruf S, Masduki FF et al (2012) The plastid genome-encoded ycf4 protein functions as a nonessential assembly factor for photosystem I in higher plants. *Plant Physiol* 159:579–591. <https://doi.org/10.1104/pp.112.196642>
- Krishnaswamy S, Verma S, Rahman MH, Kav NNV (2011) Functional characterization of four APETALA2-family genes (*RAP2.6*, *RAP2.6L*, *DREB19* and *DREB26*) in *Arabidopsis*. *Plant Mol Biol* 75:107–127. <https://doi.org/10.1007/s11103-010-9711-7>
- Kudo M, Kidokoro S, Yoshida T et al (2019) A gene-stacking approach to overcome the trade-off between drought stress tolerance and growth in *Arabidopsis*. *Plant J* 97:240–256. <https://doi.org/10.1111/tpj.14110>
- Langfelder P, Horvath S (2008) WGCNA: an R package for weighted correlation network analysis. *BMC Bioinformatics* 9:559. <https://doi.org/10.1186/1471-2105-9-559>
- Langfelder P, Luo R, Oldham MC, Horvath S (2011) Is my network module preserved and reproducible? *PLoS Comput Biol* 7:e1001057. <https://doi.org/10.1371/journal.pcbi.1001057>
- Li Y, Chu Z, Luo J et al (2018) The C2H2 zinc-finger protein SIZF3 regulates AsA synthesis and salt tolerance by interacting with CSN5B. *Plant Biotechnol J* 16:1201–1213. <https://doi.org/10.1111/pbi.12863>
- Liao Y, Smyth GK, Shi W (2014) FeatureCounts: an efficient general purpose program for assigning sequence reads to genomic features. *Bioinformatics* 30:923–930. <https://doi.org/10.1093/bioinformatics/btt656>
- Liu X-M, Nguyen XC, Kim KE et al (2013) Phosphorylation of the zinc finger transcriptional regulator ZAT6 by MPK6 regulates *Arabidopsis* seed germination under salt and osmotic stress. *Biochem Biophys Res Commun* 430:1054–1059. <https://doi.org/10.1016/j.bbrc.2012.12.039>
- Mao J-L, Miao Z-Q, Wang Z et al (2016) *Arabidopsis* ERF1 mediates cross-talk between ethylene and auxin biosynthesis during primary root elongation by regulating *ASA1* expression. *PLoS Genet* 12:e1005760. <https://doi.org/10.1371/journal.pgen.1005760>
- McGrath KC, Dombrecht B, Manners JM et al (2005) Repressor- and activator-type ethylene response factors functioning in jasmonate signaling and disease resistance identified via a genome-wide screen of *Arabidopsis* transcription factor gene expression. *Plant Physiol* 139:949–959. <https://doi.org/10.1104/pp.105.068544>
- Merelo P, Xie Y, Brand L et al (2013) Genome-wide identification of KANADII target genes. *PLoS ONE* 8:e77341. <https://doi.org/10.1371/journal.pone.0077341>
- Meyer K, Köster T, Nolte C et al (2017) Adaptation of iCLIP to plants determines the binding landscape of the clock-regulated RNA-binding protein AtGRP7. *Genome Biol* 18:204. <https://doi.org/10.1186/s13059-017-1332-x>
- Mravec J, Skůpa P, Bailly A et al (2009) Subcellular homeostasis of phytohormone auxin is mediated by the ER-localized PIN5 transporter. *Nature* 459:1136–1140. <https://doi.org/10.1038/nature08066>
- Naseem M, Kaldorf M, Dandekar T (2015) The nexus between growth and defence signaling: auxin and cytokinin modulate plant immune response pathways. *J Exp Bot* 66:4885–4896. <https://doi.org/10.1093/jxb/erv297>
- Nelson R, Wiesner-Hanks T, Wissner R, Balint-Kurti P (2017) Navigating complexity to breed disease-resistant crops. *Nat Rev Genet* 19:21–33. <https://doi.org/10.1038/nrg.2017.82>
- Nusinow DA, Helfer A, Hamilton EE et al (2011) The ELF4–ELF3–LUX complex links the circadian clock to diurnal control of hypocotyl growth. *Nature* 475:398–402. <https://doi.org/10.1038/nature10182>

- Pandey SP, Roccaro M, Schön M et al (2010) Transcriptional reprogramming regulated by WRKY18 and WRKY40 facilitates powdery mildew infection of *Arabidopsis*. *Plant J* 64:912–923. <https://doi.org/10.1111/j.1365-313X.2010.04387.x>
- Paponov IA, Paponov M, Teale W et al (2008) Comprehensive transcriptome analysis of auxin responses in *Arabidopsis*. *Mol Plant* 1:321–337. <https://doi.org/10.1093/mp/ssm021>
- Pinon V, Prasad K, Grigg SP et al (2013) Local auxin biosynthesis regulation by PLETHORA transcription factors controls phyllotaxis in *Arabidopsis*. *Proc Natl Acad Sci USA* 110:1107–1112. <https://doi.org/10.1073/pnas.1213497110>
- Ritchie ME, Phipson B, Wu D et al (2015) Limma powers differential expression analyses for RNA-sequencing and microarray studies. *Nucleic Acids Res* 43:e47–e47. <https://doi.org/10.1093/nar/gkv007>
- Sakamoto H, Araki T, Meshi T, Iwabuchi M (2000) Expression of a subset of the *Arabidopsis* Cys2/His2-type zinc-finger protein gene family under water stress. *Gene* 248:23–32. [https://doi.org/10.1016/S0378-1119\(00\)00133-5](https://doi.org/10.1016/S0378-1119(00)00133-5)
- Sakamoto H, Maruyama K, Sakuma Y et al (2004) *Arabidopsis* Cys2/His2-type zinc-finger proteins function as transcription repressors under drought, cold, and high-salinity stress conditions. *Plant Physiol* 136:2734–2746. <https://doi.org/10.1104/pp.104.046599>
- Schult K, Meierhoff K, Paradies S et al (2007) The nuclear-encoded factor HCF173 is involved in the initiation of translation of the psbA mRNA in *Arabidopsis thaliana*. *Plant Cell* 19:1329–1346. <https://doi.org/10.1105/tpc.106.042895>
- Shi H, Wang X, Ye T et al (2014) The cysteine2/histidine2-type transcription factor ZINC FINGER OF ARABIDOPSIS THALIANA6 modulates biotic and abiotic stress responses by activating salicylic acid-related genes and C-repeat-binding factor genes in *Arabidopsis*. *Plant Physiol* 165:1367–1379. <https://doi.org/10.1104/pp.114.242404>
- Strange RN, Scott PR (2005) Plant disease: a threat to global food security. *Annu Rev Phytopathol* 43:83–116. <https://doi.org/10.1146/annurev.phyto.43.113004.133839>
- Thines B, Katsir L, Melotto M et al (2007) JAZ repressor proteins are targets of the SCF^{COI1} complex during jasmonate signaling. *Nature* 448:661–665. <https://doi.org/10.1038/nature05960>
- van Dam S, Vösa U, van der Graaf A et al (2018) Gene co-expression analysis for functional classification and gene-disease predictions. *Brief Bioinform* 19:575–592. <https://doi.org/10.1093/bib/bbw139>
- Vandepoele K, Quimbaya M, Casneuf T et al (2009) Unraveling transcriptional control in *Arabidopsis* using cis-regulatory elements and coexpression networks. *Plant Physiol* 150:535–546. <https://doi.org/10.1104/pp.109.136028>
- Windram O, Madhou P, McHattie S et al (2012) *Arabidopsis* defense against *Botrytis cinerea*: chronology and regulation deciphered by high-resolution temporal transcriptomic analysis. *Plant Cell* 24:3530–3557. <https://doi.org/10.1105/tpc.112.102046>
- Xie Y, Mao Y, Lai D et al (2012) H₂ enhances *Arabidopsis* salt tolerance by manipulating ZAT10/12-mediated antioxidant defence and controlling sodium exclusion. *PLoS ONE* 7:e49800. <https://doi.org/10.1371/journal.pone.0049800>
- Xie Y, Straub D, Eguen T et al (2015) Meta-analysis of *Arabidopsis* KANADI1 direct target genes identifies a basic growth-promoting module acting upstream of hormonal signaling pathways. *Plant Physiol* 169:1240–1253. <https://doi.org/10.1104/pp.15.00764>
- Yang L, Teixeira PJPL, Biswas S et al (2017) *Pseudomonas syringae* Type III effector HopBB1 promotes host transcriptional repressor degradation to regulate phytohormone responses and virulence. *Cell Host Microbe* 21:156–168. <https://doi.org/10.1016/j.chom.2017.01.003>
- Yin M, Wang Y, Zhang L et al (2017) The *Arabidopsis* Cys2/His2 zinc finger transcription factor ZAT18 is a positive regulator of plant tolerance to drought stress. *J Exp Bot* 68:2991–3005. <https://doi.org/10.1093/jxb/erx157>

Publisher's Note Springer Nature remains neutral with regard to jurisdictional claims in published maps and institutional affiliations.